P127 A VARIATIONAL APPROACH TO RETRIEVE 3D RADAR REFLECTIVITY COMPOSITES

Jordi Roca-Sancho*, Marc Berenguer, Daniel Sempere-Torres
Centre de Recerca Aplicada en Hidrometeorologia. Universitat Politècnica de Catalunya, Barcelona (Spain).

1. INTRODUCTION

Radar networks offer the possibility to improve Quantitative Precipitation Estimation (QPE) by enlarging the total covered area and providing multiple measurements in the overlapping area. Well-known problems affecting radar QPE such as beam blockage, attenuation by intense precipitation or beam broadening with distance can be mitigated when measurements from multiple radars are available for the same area. Radar data compositing is normally performed using simply range-related or value related algorithms of selection and combination. Usual methods are: attributing to the common cell the maximum observed value, assigning the observation from the closest radar, or combining data through a weighted average based on distance. First approach handles only with attenuation, and the second and the third are based on the assumption that radar data reliability diminishes only with distance. Fornasiero et al. (2006) propose a composition technique based on quality indices for two-dimensional reflectivity fields, with high dependence on quality descriptors and without using 3-dimensional information of radar data. Zhang et al. (2005) obtain 3-dimensional reflectivity composites for the NEXRAD network in USA territory using linear interpolation to convert polar data to Cartesian data and a weighted average based on distance.

This study proposes an alternative methodology to obtain high-resolution radar reflectivity composites based on a variational approach considering different error sources in an explicit manner. The methodology retrieves the 3-dimensional precipitation field most compatible with the observations from the different radars of the network. With this aim, the methodology uses a model that simulates the radar sampling of the atmosphere. The model settings are different for each radar and include features such as the radar location, hardware parameters (beam width, pulse length…) and the scan strategy. The methodology follows the concept of an inverse method based on the minimization of a cost function that penalizes discrepancies between the simulated and actual observations for each radar. The simulation model is able to reproduce the effect of beam broadening with the distance and attenuation by intense precipitation.

The methodology has been applied on two radars close to Barcelona (Spain).

2. DATA USED IN THIS STUDY

The radar data used in this study were recorded with two C-band radars in the vicinity of Barcelona belonging to the Meteorological Service of Catalonia (SMC). The two radars are separated by 72 km and located in the Creu del Vent hill (825 m AMSL) and at the summit of La Miranda (910 AMSL, see Figure 1). Hereafter we will refer to them as CDV radar and LMI radar, respectively. Both radars follow a scanning strategy of 16 elevations with a resolution of 1 degree in azimuth and 1 km in range. CDV radar has a maximum range of 150 km and LMI radar one of 130 km. Complete volume scans are produced every 6 minutes for both radars.

We selected two instants of two different events whose data are available for both radars in order to apply our approach. A convective event occurred on the 17 and 18 September 2009 from which we extract observations made by both radars at 2006 UTC 17 September 2009. The first elevation of the observed volume scan for each radar is shown in Figures 2a and 2b, where we can see that observations of the same regions are quite different from one radar to the other. The second case is a mainly stratiform event occurred between the 4 and the 6 February 2010 and selected volume scans corresponds to 1430 UTC 4 February 2010. In both cases radar data have been corrected for ground clutter and beam blockage before its usage. This is because our approach focuses on mitigate beam broadening and attenuation by intense precipitation and assumes no interception of the beam with the terrain.

Reflectivity composites are carried out in a 3-dimensional Cartesian grid inside the overlapping region where both radars take measurements. This Cartesian domain has dimensions of 75 km eastward, 75 km northward and 7 km in altitude, with a resolution of 250 meters in each direction. The area covered by this grid includes both radar locations.

Currently, the composition technique operationally implemented at the Meteorological Service of Catalonia (SMC) is assigning to each point covered by more than one radar the maximum observed value. In this document, we will refer to this approach as the *maximum value technique*.

Figure 1. Illustration of radar locations.

Corresponding author address: Jordi Roca-Sancho, CRAHI-UPC Gran Capità 2-4 Ed. Nexus D-104. E08034-Barcelona (Spain). e-mail: jordi.roca@crahi.upc.edu

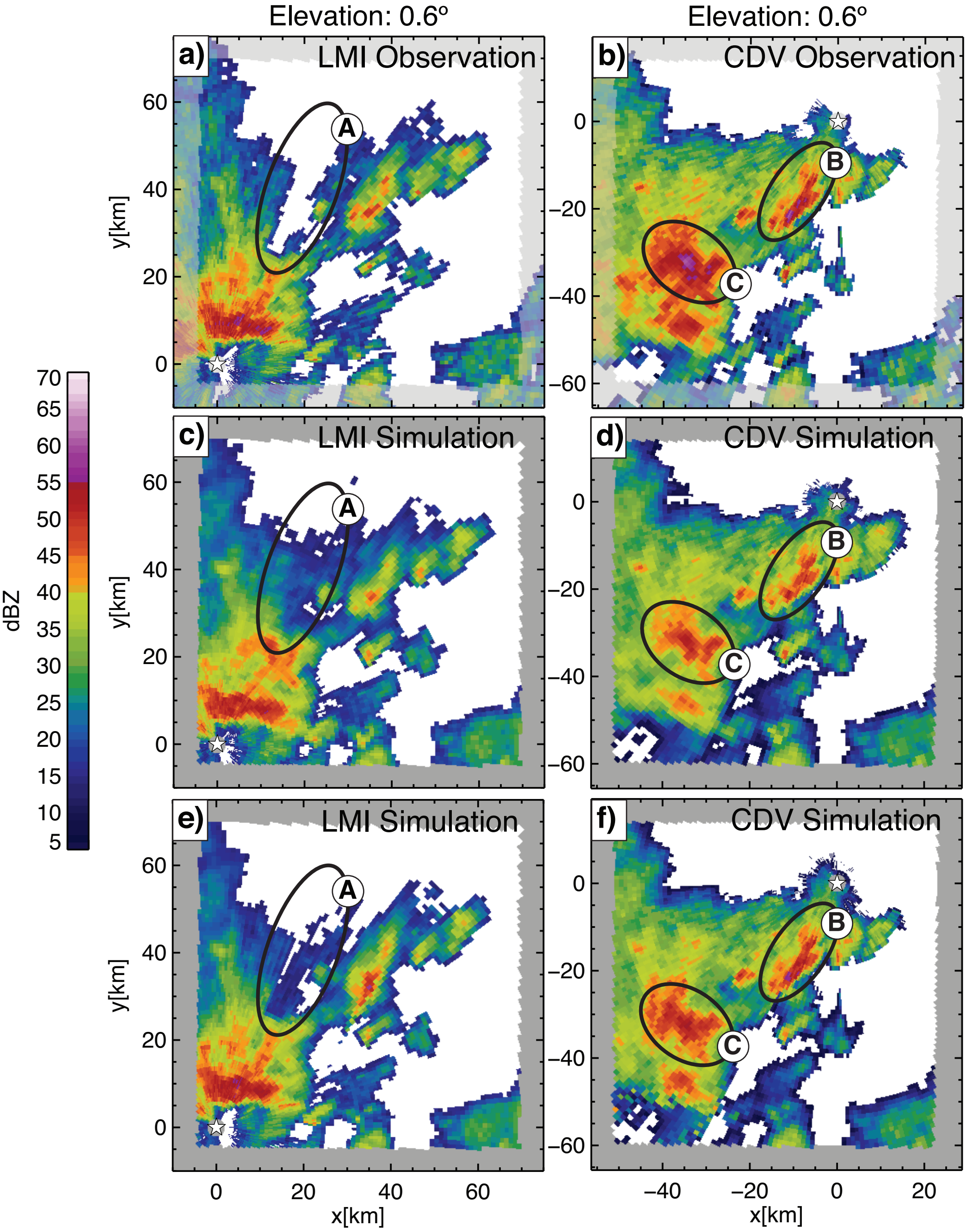

Figure 2. First row: first elevation of the volume scan recorded by LMI (a) and CDV (b) radars at 2006 UTC 17 September 2009. Second row: first elevation of the simulated scan over the 3-dimensional precipitation field obtained using the maximum value technique for (c) the LMI radar and (d) the CDV radar. Third row: first elevation of the simulated scan over the 3-dimensional precipitation field retrieved using the variational approach for (e) the LMI radar and (f) the CDV radar. Shaded areas in observations and gray areas in simulations correspond to region outside the domain. Region A on the LMI observation (a) shows an attenuation corridor that is not reproduced by simulation over the field obtain by maximum value technique (c) but is reproduced by simulation over the retrieved field (e). Labels B and C on CDV observation (b) indicate convective cells better reproduced using the retrieved field (f) than using the field obtained by maximum value technique (d) despite high values in cell C are not achieved.

3. VARIATIONAL APPROACH

The retrieval technique is based on the minimization of a cost function that penalizes the discrepancies between actual observations and simulations performed over the retrieved field. We define the cost function as:

$$F(Z) = \left\| R_{LMI} - \hat{R}_{LMI}(Z) \right\|^2 + \left\| R_{CDV} - \hat{R}_{CDV}(Z) \right\|^2 \qquad (1)$$

Where Z is the retrieved high-resolution 3D reflectivity field, R_{LMI} is the reflectivity volume scan observed with the LMI radar and $\hat{R}_{LMI}(Z)$ is the simulated reflectivity volume scan for the LMI radar, R_{CDV} and $\hat{R}_{CDV}(Z)$ are the observed and simulated volume scans for CDV radar and $\left\| R - \hat{R}(Z) \right\|$ stands for Euclidean distance between observation and simulation.

The cost function is minimized iteratively with the Conjugate Gradient method to retrieve the 3-dimensional composite.

3.1 Simulation model

Simulations are carried out using a model that reproduces the radar sampling of the atmosphere considering radar characteristics (location, beam width, pulse length…), scan strategy, power distribution within the radar beam and attenuation by precipitation, similarly as in Llort et al. (2006).

Given a 3-dimensional precipitation field, a complete volume scan is generated by the model. The simulation model is based in the radar equation (2).

For a certain elevation and a certain azimuth the radar equation (2) expresses the received power from range r, $P(r)$, as a function of the high-resolution 3D reflectivity field Z:

$$P(r) = \frac{C}{r^4} \int_{V(r)} |W|^2 f^4 Z_m dV$$

$$Z_m(r) = Z(r) \cdot \exp\left(-0.2 \ln(10) \int_0^r \alpha \cdot Z(s)^\beta \, ds \right) \qquad (2)$$

Where C is a constant related to the radar characteristics, $V(r)$ is the radar sampling volume at range r, $|W|^2$ is the range weighting function –in this model the function proposed by Doviak and Zrnic (1992) is used-, f^4 is the normalized power –which is approximated by a Gaussian function-, Z_m is the measured (attenuated) reflectivity and α and β are parameters of a power law relationship between specific attenuation and reflectivity ($k = \alpha \cdot Z^\beta$).

This equation allows to reproduce the effect of the power distribution within the beam, the effect of beam broadening and signal attenuation by precipitation.

3.2 First guess

A first guess of the 3-dimensional precipitation field is needed to initialize the iterative minimization. We obtain this first guess from observations of both radars by means of the maximum value technique. With this aim, observations of each radar are converted from polar coordinates to the common 3-dimensional Cartesian grid introduced above (75x75x7 km^3, 250m-resolution). The conversion is done by the nearest neighbor algorithm that is the best choice to preserve extreme values and small-scale variability (Trapp and Doswell 2000). This process is illustrated in Figure 3.

Figures 2c and 2d show the simulations of the first elevation obtained by applying equation 2 to field obtained by maximum value technique. We can see that for the LMI radar, the simulation does not reproduce the attenuation corridor in the observation (labeled as A in Figure 2a and 2c). For CDV radar convective cells are in general less intense in the simulation than observed (as in labels B and C in Figures 2b and 2d).

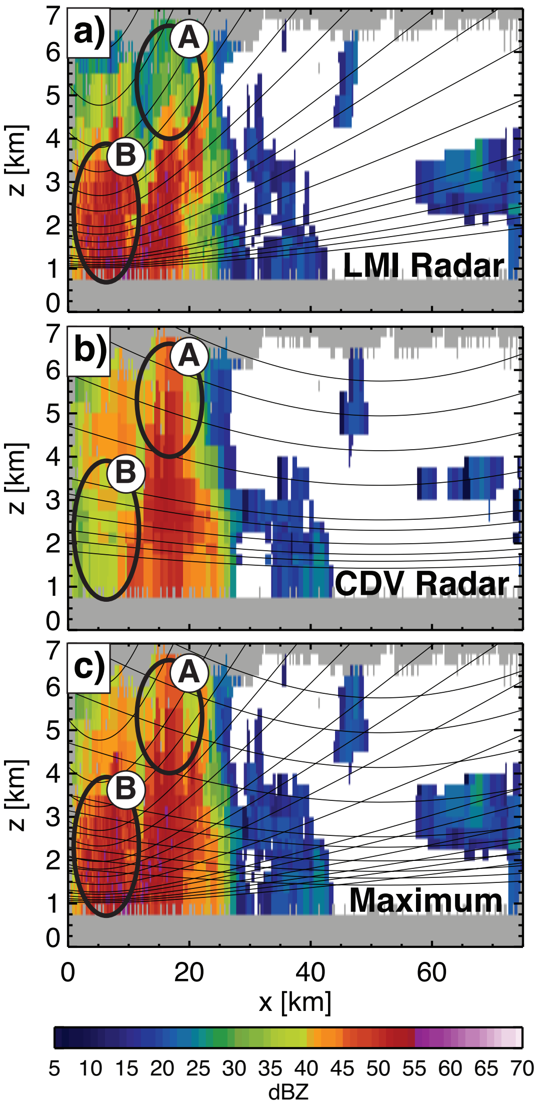

Figure 3. A vertical cross section of the precipitation field obtained by the nearest neighbor algorithm for (a) LMI and (b) CDV radar observations of the 17 September 2009 2006 UTC. The (c) field is generated from the two above by the maximum value technique. Thin lines represent the path of the radar ray. In region labeled as A the field obtained by maximum value technique is dominated by the CDV radar, while in region labeled as B LMI radar is dominant.

4. RESULTS

The presented variational approach has been applied to LMI and CDV radars for the two cases described in Section 2.

4.1 Convective Case

In the convective case (2006 UTC 17 September 2009) the retrieved 3-dimensional precipitation field is presented in Figure 4. We can see that the convective cell in region A has a vertical development that exceeds the height of 6 km while the one in region B reaches the height of 5 km approximately.

Figures 2e and 2f show the simulations for both radars obtained by applying equation 2 on the retrieval. Visual comparison of Figures 2a and 2b with Figures 2e and 2f shows that the similarity between actual observations and simulations is remarkable. For example is worth pointing certain features at the field:

- The LMI simulation reproduces quite well the attenuation corridor (labeled as A in Figures 2a and 2e).
- CDV simulations show that the convective cell labeled as B is better reproduced using the retrieved field than using the field obtained by maximum value technique (compare simulations in Figures 2d and 2f with observation in Figure 2b).
- High reflectivity values in the convective cell labeled as C are the clearest difference between CDV observation and CDV simulation (Figure 2b versus 2f). Such high observed reflectivity values could perhaps be attributed to the presence of hail which is not considered in this approach.

This similarity illustrates that the retrieved field is the most compatible with both observations as the statement of the problem claims.

4.2 Stratiform case

Radar observations used for the stratiform case are shown in Figures 5a and 5b. The field retrieved by the methodology is presented in Figure 6. In this stratiform case, we expected to see a clear bright band in vertical cross sections (Figures 6d, 6e and 6f) but only small evidence of it can be found (see label A of Figure 6d at the height of 2km). Further investigation is required at this point. The simulations over the retrieved field (Figures 5c and 5d) are quite similar to observations.

Analysis of first elevation observed by both radars seems to show in general higher intensities in CDV observation than LMI observation (compare Figures 5a and 5b). Such difference may be due to a difference in calibration between the two radars. Miscalibration is not considered in this approach and will be included in future experiments.

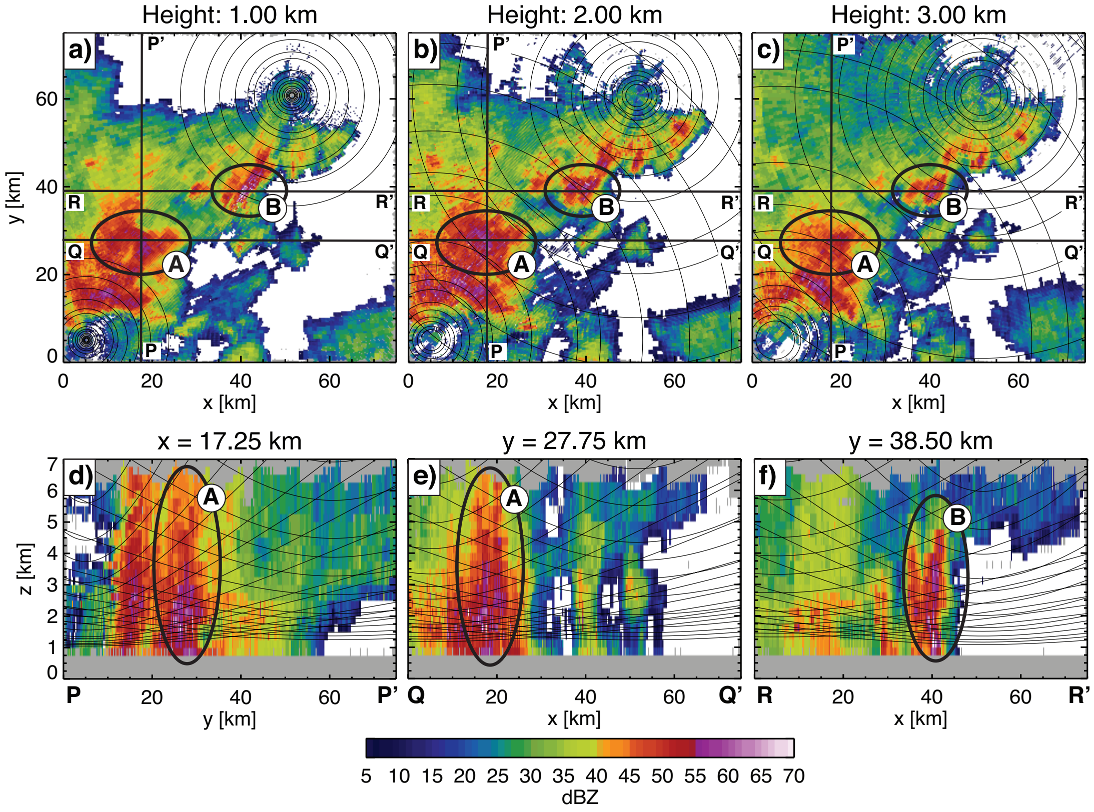

Figure 4. CAPPIs of the 3-dimensional precipitation field retrieved by variational approach for the heights of 1, 2, and 3 km (panels (a), (b) and (c) respectively) and vertical cross sections of the same 3-dimensional precipitation field keeping constant coordinate x (at 17.25 km, panel (d)) and coordinate y (at 27.75 km and 38.50 km, panels (e) and (f) respectively). Thin lines correspond to the path of radar ray for each elevation and straight thick lines in the top panels indicate the situation of vertical cross sections represented in bottom panels. Gray areas correspond to regions not covered by radar scans (in altitudes lower than 1 km) or to sampling volumes partially outside of the domain (in higher altitudes). The field corresponds to 2006 UTC 17 September 2009. In region A there is a convective cell, its vertical development can be seen in both panels (d) and (e). A smaller convective cell is shown in region B.

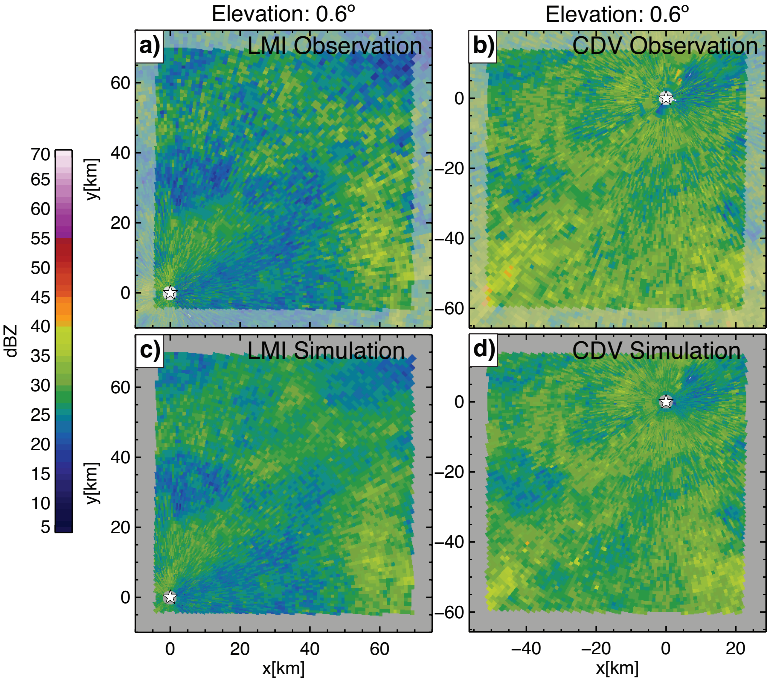

Figure 5. Top: first elevation of the volume scan recorded by LMI (a) and CDV (b) radars the 4 February 2010 1430 UTC. Bottom: first elevation of the simulated volume scan over the retrieved field for (c) the LMI radar and (d) the CDV radar. Shaded areas in observations and gray areas in simulations correspond to region outside the domain.

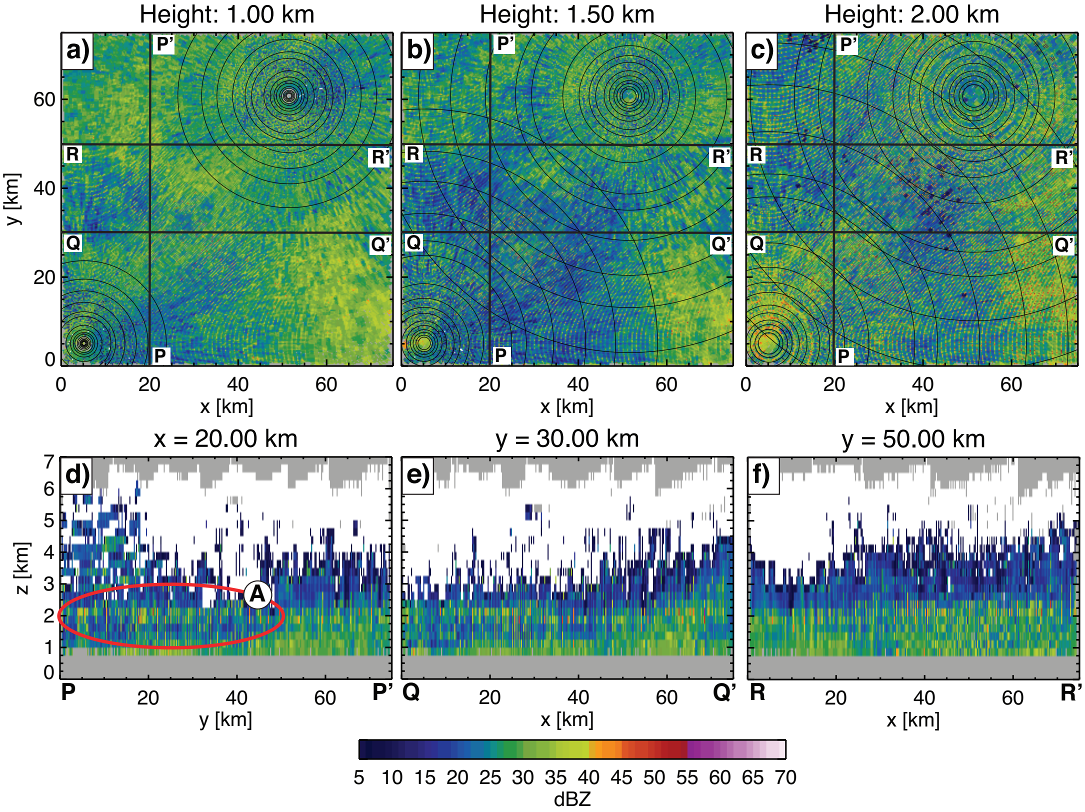

Figure 6. CAPPIs of the 3-dimensional precipitation field retrieved by variational approach for the heights of 1, 1.5, and 2 km (panels (a), (b) and (c) respectively) and vertical cross sections of the same 3-dimensional precipitation field keeping constant coordinate x (20 km, panel (d)) and coordinate y (at 30 km and 50 km, panels (e) and (f) respectively). Thin lines corresponds to the path of radar ray for each elevation and straight thick lines in the top panels indicate the situation of vertical cross sections represented in bottom panels. Gray areas correspond to regions not covered by radar scans (in altitudes lower than 1 km) or to sampling volumes partially outside of the domain (in higher altitudes). The field corresponds to 1430 UTC 4 February 2010. In region A can be seen the bright band enhancement at a height of 2 km.

5. CONCLUSION

A methodology based on a variational approach to retrieve 3-dimensional reflectivity composites has been presented. Knowledge on radar measurements has been included in the approach by simulating radar observation at precipitation.

We have presented preliminary results for two different rainfall cases. Reflectivity composites obtained in this work reproduce the vertical development of convective cells but do not achieve a clear representation of the bright band. Qualitative comparison between observations and simulations are used to assess the consistency of the results.

To complete the work presented here, a more quantitative and systematic verification will be carried out in the forth-coming work, comparing retrieved precipitation fields against an external source of information, as rain gauges or other radars.

Acknowledgements: This work has been carried out in the framework of the project ProFEWS (CGL2010-15892) funded by the Spanish Science and Innovation Ministry (MICINN). The first author is also grateful to the MICINN for the FPI scholarship BES-2008-005217 associated to the project ESP2007-62417.

References

Doviak, R. J., and D. S. Zrnic, 1992: *Doppler radar and weather observations.* 2nd ed. Academic Press, 562 pp.

Fornasiero, A., P. P. Alberoni, R. Amorati, and C. Marsigli, 2006: Improving the radar data mosaicking procedure by means of a quality descriptor. *Fourth European Conference on Radar in Meteorology and Hydrology*, Barcelona, Spain, 378-381.

Llort, X., M. Berenguer, R. Sánchez-Diezma, and D. Sempere-Torres, 2006: Analysis of the radar distance error structure through a simulation approach. *Fourth European Conference on Radar in Meteorology and Hydrology (ERAD)*, Barcelona, Spain, 567-574.

Trapp, R. J., and C. A. Doswell, 2000: Radar Data Objective Analysis. *Journal of Atmospheric and Oceanic Technology*, **17,** 105-120.

Zhang, J., K. Howard, and J. J. Gourley, 2005: Constructing Three-Dimensional Multiple-Radar Reflectivity Mosaics: Examples of Convective Storms and Stratiform Rain Echoes. *Journal of Atmospheric and Oceanic Technology*, **22,** 30-42.